NOVEL LEAD-LAG COMPENSATOR FOR MAGNET CORRECTION POWER SUPPLY OF TPS

Yong-Seng Wong, Chen-Yao Liu*, Kuo-Bin Liu, Yuan-Chen Chien
and Bao-Sheng Wang

Department of Power Supply Group
National Synchrotron Radiation Research Center
No. 101, Hsin Ann Road, Hsinchu 300, Taiwan
wong.ys@nsrrc.org.tw; *Corresponding author: cyl@nsrrc.org.tw

Abstract. *Taiwan Photon Source (TPS) is the most important project of the Taiwanese government. From 2012 to 2016, the total budget of TPS amounted to over US210 million. It set up a synchrotron storage ring (electron energy of 3.3 GeV, circumference of 518 m, and low emittance) that provides one of the world's brightest synchrotron sources of x-rays. This study presents a novel analysis and design of compensators for magnet corrector power supply to avoid limitations in stabilizing the frequency when the machine output current load is valid. A lead-lag compensator had been built in a full-bridge converter to improve the system bandwidth. Lead-lag compensators influence various disciplines, such as robotics, satellite control, automobile diagnostics, and laser frequency stabilization. These components are important building blocks in analog control systems and can also be used in digital control. A 50 V output voltage and 10 A output current prototype converter is fabricated in the laboratory. Furthermore, the gain and phase margins experiments verify the effectiveness of the control loop design approach.*
Keywords: Compensator, Gain margin, Phase margin, Corrector, Lead-lag compensation

1. **Introduction.** A light source must maintain a considerably precise current at the operation steady state. Therefore, a few correction magnets are required for the accelerator power supply (APS) machine to correct the beam [1-3]. For the Taiwan Photon Source (TPS) project, the quadrupole magnets of the storage ring have the most significant effect on the stability of the positron closed orbit as a result of the low frequency vibration [4,5]. Correction magnets are distributed around the injector synchrotron ring. These magnets provide the field changes required for the beam orbit correction during the acceleration period at the rate of 2 Hz. Since the exact field correction required at each correction magnet location will not be known until a beam is actually accelerated, an arbitrary function generator (AFO) is required to produce a correction field. Therefore, a high-precision bipolar corrector (i.e., a multi-channel corrector magnet driver system) has been designed and is capable of providing precision bipolar output currents with minimal zero-crossover distortion. However, the magnet corrector power supply has been limited to stabilize the frequency when the machine output current load is valid. A compensator should be designed to observe the circuit gain and phase margins [6-9]. Figure 1 shows the machine control block. The power modules are controlled using −10 V to +10 V analog command signals, thereby enabling the comparison of the feedback signal from the output current. Therefore, the error amplifier can provide a pulse width modulation (PWM) signal to control the power switch. The correction field required can either be positive or negative; thus, for all the correction magnets, bipolar power supplies are required to produce both polarities of the correction fields [10,11]. Figure 2 shows that magnet correction power supply (MCPS) uses a custom H-bridge configuration. The overlapping
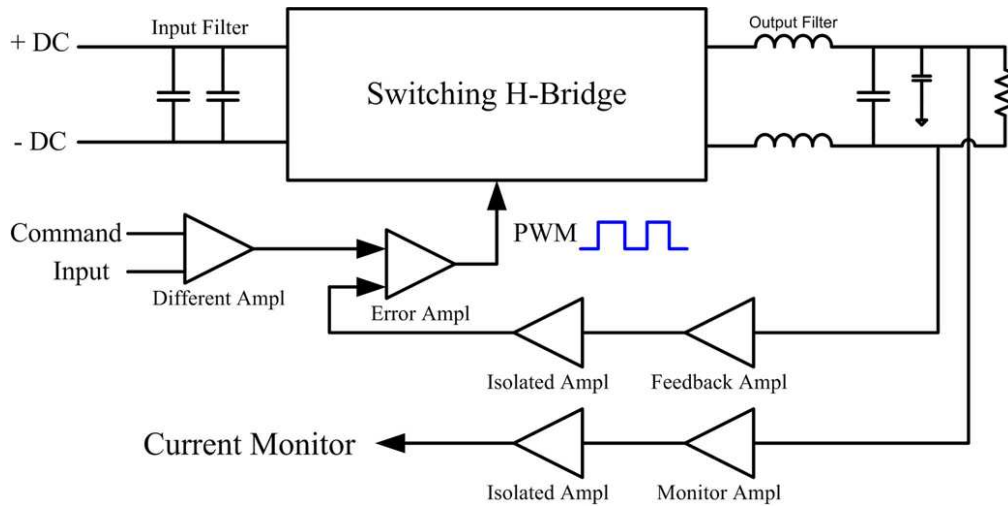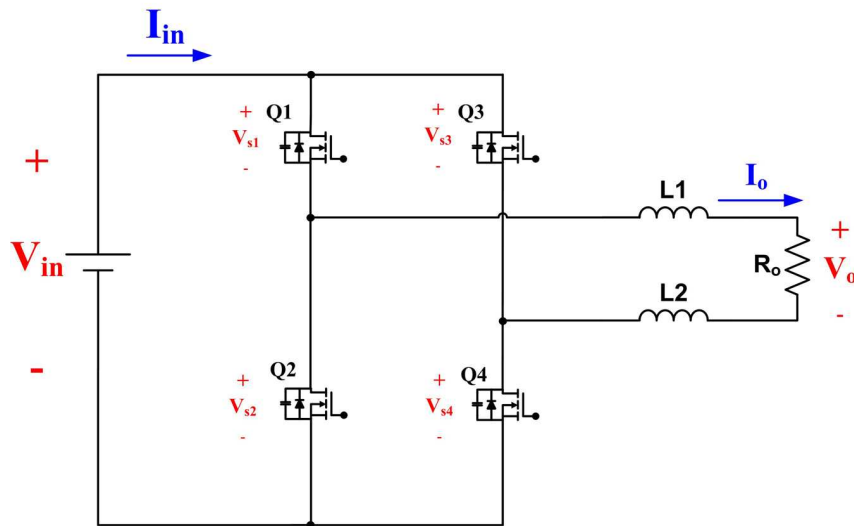
FIGURE 1. Correction power supply block diagram

FIGURE 2. Correction power supply equivalent circuit

volt-seconds feedback mode is used instead of a straight voltage mode to achieve a substantially high control bandwidth, as well as the correction power supply output current, by controlling the pulse width of an H-bridge DC-DC power converter [12,13]. For the positive magnet current, the Q1 and Q4 switches are turned on and the input DC voltage supplied energy to the output magnet load. However, for the negative magnet current, the Q2 and Q3 power switches are turned on and the output magnet load obtained a negative current. The output feedback controller is used for the 4-terminal Kelvin connection magnet shunt resistors, which has a high-precision output current. These are 10 milliohm shunts that have an absolute tolerance of 0.1%, thereby ensuring output current noise under 100 u Arms at high load conditions (30 A). This corrector power converter could output current with 5 ppm stability within 15 hours, 20 uA ripple (0 ∼ 1 kHz) and with suitable tuning on PI parameter of error amplifier, 1.5 kHz high frequency response bandwidth is reached. This corrector magnet power converter is versatile to meet any kind of requirements for magnets to be powered within ±10 amperes that include booster ring corrector (horizontal & vertical), trim coil of storage ring sextupole magnet (include horizontal dipole, vertical dipole & skew quadrupole) and fast feedback corrector. By using this power converter could save a lot of work in maintenance and quantity of spare parts is minimized.
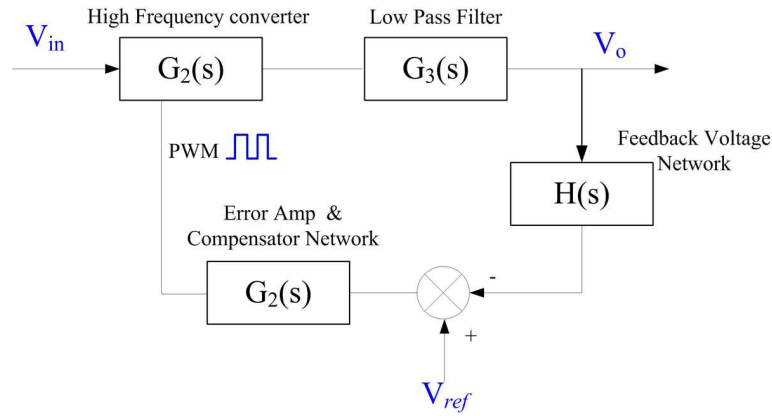
FIGURE 3. Correction power supply equivalent circuit

2. **Correction Power Supply Open-loop Gain and Phase Margins.** Linear time-invariant systems with different frequency sine wave signal input systems explore the amplitude gain and phase response to changes in the relationship between the input and output. Thus, the frequency response is obtained. All the switch power supplies are designed in a compensator in the frequency domain, thereby generally satisfying the specifications on steady-state accuracy and phase margin. Figure 3 shows the block diagram of a control scheme of a correction magnet power supply, and the feedback voltage through the output voltage divided the resistance into the adder signal. The feedback signal and refer voltage signal to sum are compared with the pulse width modulation (PWM) signal and into the power switch transfer with error amplifier and compensator. ω_c is the cross frequency with MCPS. The closed-loop control function gain and phase margins can be written as follows:

$$\text{Gain Margin} = 20 \log_{10} \frac{1}{G(j\omega_c) H(j\omega_c)} \tag{1}$$

$$\text{Phase Margin} = 360° + \angle G(j\omega_g) H(j\omega_g) \tag{2}$$

MCPS and cross frequencies are set at 24.5 kHz and 5 kHz, respectively. The experiments and plots presented in this study are performed using Simplis software. The experimental result measurements are obtained from the various output current data.

This study uses a dynamic signal analysis of 35670 A scan from 51.2 Hz to 51.2 kHz frequency response with MCPS (Figure 4). The gain margin (red line) is the decay at 20 dB/dec and the initial value is 27.63 dB, and the cross frequency (4.5 kHz) is – 6.86 dB and 0 dB at 2.67 kHz. Meanwhile, the machine phase margin is 57°. The compensator network can increase the gain and phase margins of the converter power system. A Nyquist plot is used in the automatic control and signal processing to assess the stability of a system with feedback. It is represented by a graph in polar coordinates, in which the gain and phase of a frequency response are plotted. Figure 5 shows the MCPS open-loop control system Nyquist plot curve. The maximum distance for the point of origin is 24.07 at 51 Hz, and the cross frequency is 1.016 at 2.67 kHz.

3. **Design Procedure for the Compensator.** Figure 6 illustrates the proposed compensator network equivalent circuit. The proposed compensator circuit comprises three capacitors ($C_1 \sim C_3$) and three resistors ($R_1 \sim R_3$) for the integrator and differentiator. An integrator is a form of first-order low-pass filter, which can perform in the continuous-time (analog) domain or approximated (simulated) in the discrete-time (digital) domain. An integrator has a low-pass filtering effect, but when given an offset, it will accumulate a value until it reaches a limit to the system or overflows. A differentiator circuit uses a simple first-order high-pass filter with the cut-off frequency set to be considerably above
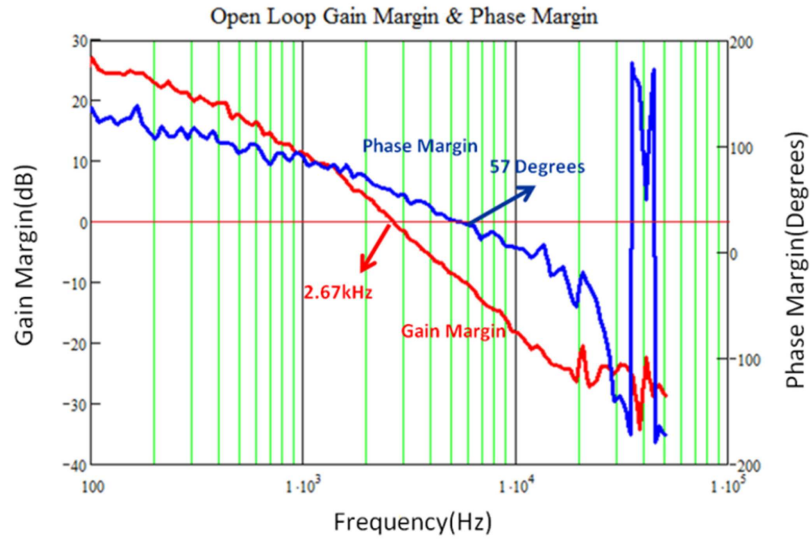
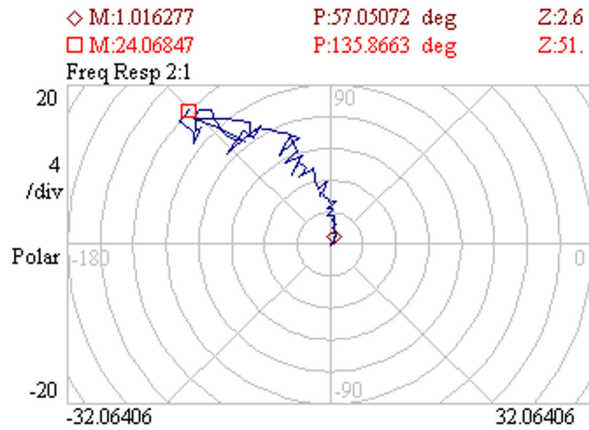FIGURE 4. Open-loop transfer function control to output bode plot

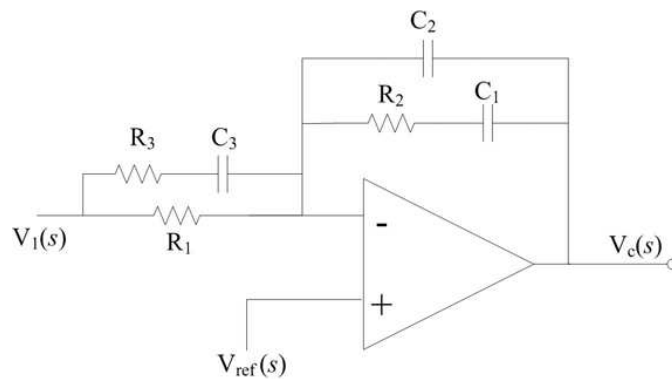FIGURE 5. Open-loop control to output Nyquist plot

FIGURE 6. Compensator lead-lag equivalent circuit

the highest frequency in the signal. The proposed compensator transfer function can be written as follows, where s is the **complex frequency** $s = \sigma + j\omega$:

$$\frac{V_c(s)}{V_1(s)} = \frac{(1 + SC_2R_2)(1 + SC_1R_1)}{(SC_2R_1)(1 + SC_1R_3)} \tag{3}$$

The zero and plot frequencies can be calculated as follows based on Equation (3):

$$f_{z1} = \frac{1}{2\pi C_1 R_2} \tag{4}$$

$$f_{z2} = \frac{1}{2\pi C_3 R_1} \tag{5}$$

$$f_{p1} = f_{\text{cross}} \tag{6}$$

$$f_{p2} = \frac{1}{2\pi C_3 R_3} \tag{7}$$

$$f_{p3} = \frac{1}{2\pi C_2 R_2} \tag{8}$$

Equations (4)-(8) show the setting component parameter of the resistor and capacitor: $R_1 = 5.1$ kΩ, $R_2 = 240$ kΩ, $R_3 = 360$ Ω and $C_1 = 200$ nF, $C_2 = 33$ pF, and $C_3 = 270$ pF. The zero and plot frequencies are $f_{z1} = 33$ Hz, $f_{z2} = 115.6$ kHz, $f_{p1} = 4.5$ kHz, $f_{p2} = 20$ kHz, and $f_{p3} = 1.64$ MHz. Figure 7 illustrates the experimental result gain and phase margins of the proposed lead-lag compensator.
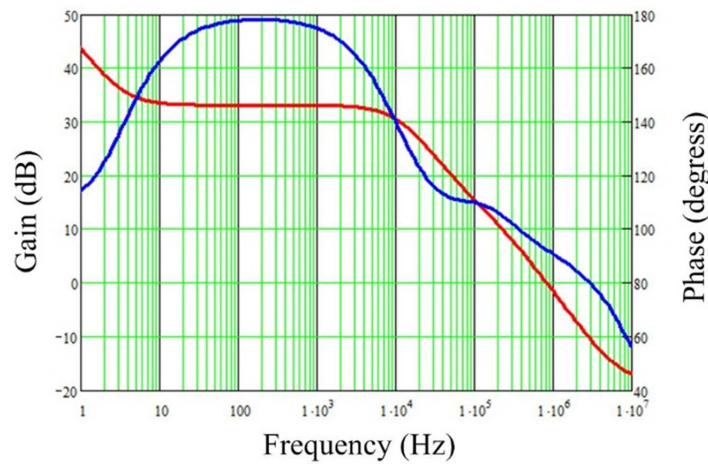

FIGURE 7. Simulation compensator lead-lag equivalent circuit gain margin and phase margin curve

4. **Experimental Result of the Bandwidth and Current Stability.** Figures 8 and 9 show the comparison of the closed- and open-loop transfer function control with the output gain and phase margins. The first plot frequency is set at 4.5 kHz to measure the MCPS stability in the current feedback control. The initial value of the closed-loop phase margin is 26.83 dB and the decay is 20 dB/dec. The gain margin is 0 dB at a cross frequency of 4.56 kHz. This gain margin is higher than that in the open-loop control, which is 0 dB at 2.67 kHz. The phase margin is 36.5° and decade to 23.5° in the first plot frequency of the system. Figure 10 shows the MCPS closed-loop control system Nyquist plot curve. The maximum distance for the point of origin is 21.80 at 54 Hz and cross frequency is 1.002 at 4.56 kHz.

Figure 11 shows the comparison between the bandwidth with compensator and the non-compensator on MCPS. The non-compensator system initiation values are from 10 dB decade to 7 dB at 60 Hz, whereas the additional compensator decade is 7 dB at 180 Hz. The bandwidth of MCPS had been increased to 120 Hz. Lastly, the proposed compensator is built in a 50 V output voltage and 10 A output current prototype converter that was fabricated in the laboratory.

Following the filter stage are four precision 4-terminal Kelvin connection Manganin shunt resistors. These 10 milliohm shunts have an absolute tolerance of 0.1%, and a
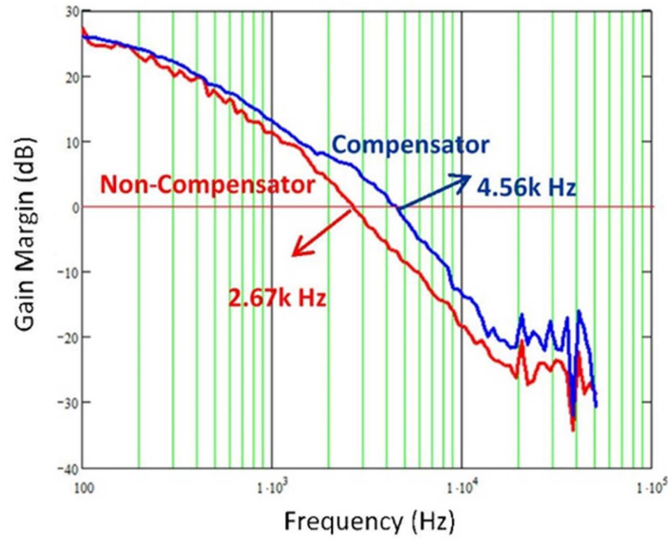
FIGURE 8. Open- and closed-loop control to output gain margin bode plot
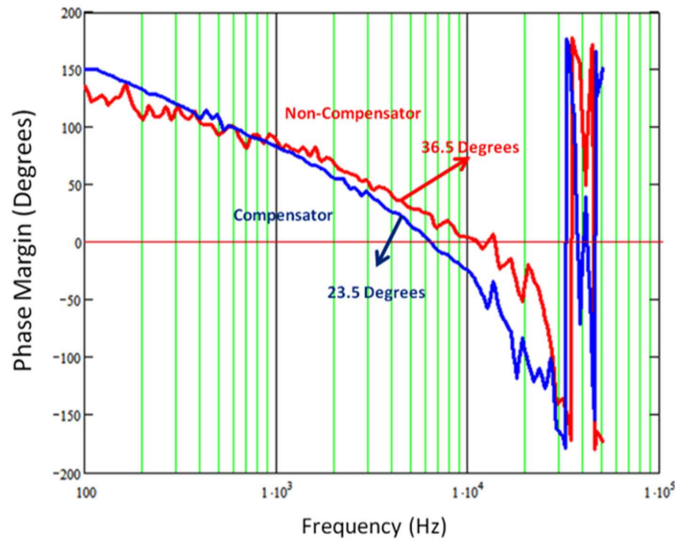

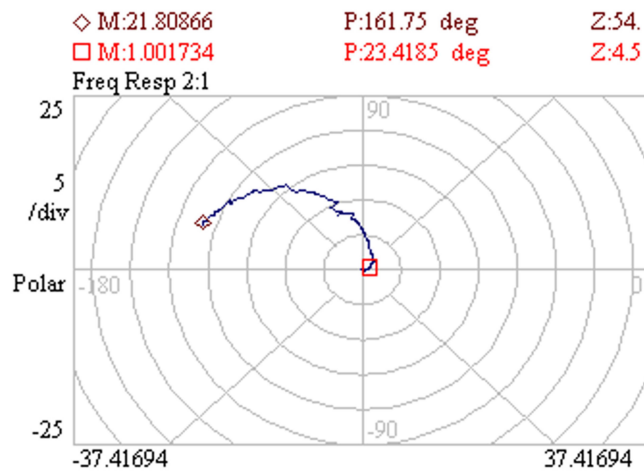FIGURE 9. Open- and closed-loop control to output phase margin bode plot

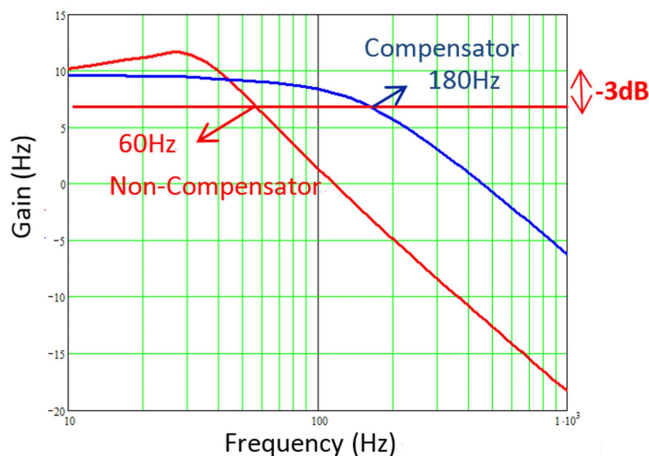FIGURE 10. Closed-loop control to output Nyquist plot

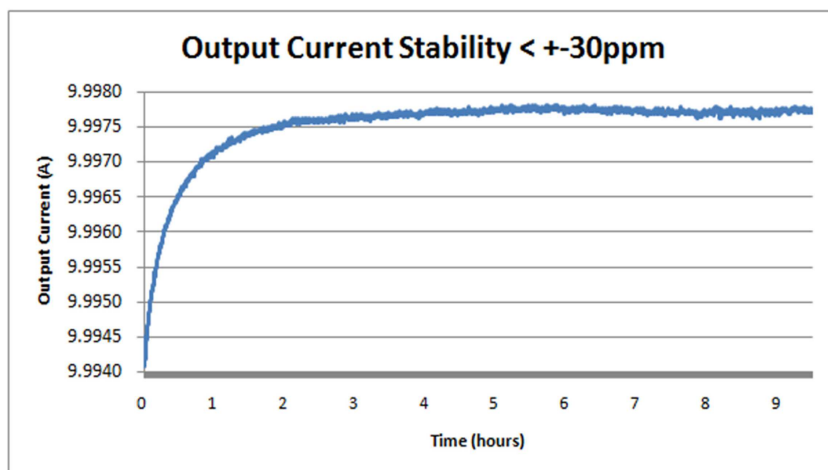FIGURE 11. Compensator and non-compensator bandwidth curve

FIGURE 12. Long-term current ripple testing

typical temperature stability of 13 ppm/°C. The input power system uses a Chroma 62075 H-30E and Keithley 263 calibrator source supply in a high-precision voltage refer signal to adjust the output current. Output loading is a pure resistor and the value is 0.25 omh. A high-precision multi-meter to long-term (9 hours and up) is used to measure the current ripple of the output current of 10 A full loading testing on MCPS. Figure 12 shows the current ripple of MCPS under ±30 ppm at long team testing.

5. **Conclusion.** The proposed lead-lag compensator has been experimentally verified, and the result has shown good agreement with the predicted values. For this study, the corrector magnet power supply bandwidth increased to 120 Hz at 7 dB to 0 dB, thereby enabling the operation at a considerably high frequency region. The advanced corrector magnet power supply improved the stability of the output current, and the output current ripple was within ±30 ppm at full load testing. The output current stabilization effectively adjusted the position of the light beam. Therefore, the corrector magnet power supplier can be used in a variety of applications, such as industrial robotics, motor control systems, high-energy physics experiments, and medical application. Lastly, a prototype circuit of the proposed corrector magnet power supply with an input voltage of 48 V, output current of 10 A, and with a maximum of 500 W is constructed in the laboratory. For the future work we expect increasing requirements from highly dynamic applications, PSI digital power electronics controller, which allows more complex control algorithms and

higher sampling rates and compare them with the dynamic performance obtained using standard PI control.

REFERENCES

[1] H. Sato, T. Shintomi, T. Ise, Y. Miura, S. Nomura and R. Shimada, Application of energy storage system for stabilization of accelerator magnet power supply, *IEEE Trans. Applied Superconductivity*, vol.20, no.3, pp.1312-1315, 2010.

[2] R. Visintini, S. Cleva, M. Cautero and T. Ciesla, A new concept of controller for accelerator' magnet power supplies, *IEEE Trans. Nuclear Science*, vol.63, no.2, pp.849-853, 2016.

[3] L. R. Yurner, S. H. Kim and K. M. Thompson, Computation of a quadrupole magnet for the APS storage ring, *IEEE Trans. Magnetics*, vol.27, no.5, pp.4231-4234, 1991.

[4] T. Takayanagi, K. kanazawa, T. Ueno, H. Someya, H. Harada, Y. Irie, M. Kinsho, Y. Yamazaki, M. Yoshimoto, J. Kamiya, M. Watanabe, M. Kuramochi and K. Satou, Improvement of the shift bump magnetic field for a closed bump orbit of the 3-GeV RCS in J-PARC, *IEEE Trans. Applied Superconductivity*, vol.18, no.2, pp.306-309, 2008.

[5] A. Napier, S. Gayadeen and S. R. Duncan, Fast orbit beam stabilisation for a synchrotron, *IEEE International Conference on Control Applications*, pp.1094-1099, 2012.

[6] Md. TausifAhmad, N. Kumar and B. Singh, Fast multilayer perceptron neural network-based control algorithm for shunt compensator in distribution systems, *IET Generation Transmission & Distribution*, vol.10, no.15, pp.3824-3833, 2016.

[7] M. Salehtavazoei and M. Tavakoli-kakhki, Compensation by fractional-order phase-lead/lag compensators, *IET Control Theory & Applications*, vol.8, no.5, pp.319-329, 2014.

[8] C. F. Lu, C. H. Hsu and C. F. Juang, Coordinated control of flexible AC transmission system devices using an evolutionary fuzzy lead-lag controller with advanced continuous ant colony optimization, *IEEE Trans. Power Systems*, vol.28, no.1, pp.385-392, 2013.

[9] A. S. Tucker, R. M. Fox and R. J. Sadleir, Biocompatible, high precision, wideband, improved howland current source with lead-lag compensation, *IEEE Trans. Biomedical Circuits and Systems*, vol.7, no.1, pp.63-70, 2013.

[10] C. Rodrigues and A. R. Silva, A new model of bipolar power supplies for LNLS steering magnets using full-bridge topology, *XI Brazilian Power Electronics Conference*, pp.1004-1008, 2011.

[11] R. Bondade, Y. Wang and D. Ma, Design of integrated bipolar symmetric output DC-DC power converter for digital pulse generators in ultrasound medical imaging systems, *IEEE Trans. Power Electronics*, vol.29, no.4, pp.1821-1829, 2014.

[12] S. H. Chen, K. L. Lin, S. S. Ng, T. C. Huang, K. H. Chen, Y. H. Lin, T. Y. Tsai and C. C. Lee, Embedded single-inductor bipolar-output DC-DC converter in class-D amplifier for low common noise, *IEEE Trans. Power Electronics*, vol.31, no.4, pp.3106-3117, 2016.

[13] D. Zhang and D. L. Zhang, Flexible-structured phase-shifted multiple-full-bridge DC-DC power supply with wide range output, *IET Power Electronics*, vol.9, no.1, pp.132-141, 2016.